JOURNAL OF GEOPHYSICAL RESEARCH, VOL. 112, D20211, doi:10.1029/2007JD008688, 2007

Aerosol forcing, climate response and climate sensitivity in the Hadley Centre climate model

Andy Jones,[1] James M. Haywood,[1] and Olivier Boucher[1]

Received 22 March 2007; revised 6 July 2007; accepted 31 July 2007; published 30 October 2007.

[1] An atmosphere/mixed-layer-ocean climate model is used to investigate the climate responses to forcing by 1860–2000 changes in anthropogenic sulfate, biomass-burning and black carbon aerosols, and how they compare with the effect of doubling CO_2. While the patterns of temperature response from sulfate and black carbon aerosols are similar and reveal high sensitivity at high latitudes in the northern hemisphere, they are significantly different to that due to CO_2 which shows high latitude sensitivity in both hemispheres, and to biomass-burning aerosols which shows a much more uniform temperature response. Climate sensitivity, the response of natural primary aerosols, and the degree to which forcings and responses are additive, are also investigated. The sum of the separate temperature and precipitation responses to each aerosol is found to be remarkably similar to that obtained if all aerosols are changed simultaneously.

Citation: Jones, A., J. M. Haywood, and O. Boucher (2007), Aerosol forcing, climate response and climate sensitivity in the Hadley Centre climate model, *J. Geophys. Res.*, *112*, D20211, doi:10.1029/2007JD008688.

1. Introduction

[2] The Intergovernmental Panel on Climate Change suggests that climate change is driven by a host of anthropogenic and natural forcing mechanisms [*IPCC*, 2007]. The relative importance of these mechanisms upon global temperature change are quantified by the radiative forcing, which essentially measures the radiative perturbation at the tropopause in units of Wm^{-2}. Increases in carbon dioxide concentrations owing to anthropogenic activity exert the strongest radiative forcing, with present-day forcing estimated at approximately 1.66 Wm^{-2} with an uncertainty spanning the range 1.5 to 1.8 Wm^{-2}. The direct radiative effect due to increases in anthropogenic aerosols is estimated as -0.5 Wm^{-2} with an uncertainty spanning the range -0.1 to -0.9 Wm^{-2}, and the first indirect effect of aerosols is estimated as -0.7 Wm^{-2} with an uncertainty spanning the range -0.3 to -1.8 Wm^{-2} [*IPCC*, 2007]. Thus although the direct and indirect effects of aerosols are considerably more uncertain than that due to carbon dioxide, they must be considered significant.

[3] Many studies have modeled the climate response to various radiative forcing mechanisms utilizing results either from atmosphere/mixed-layer-ocean models run to equilibrium or from fully coupled atmosphere/ocean models [e.g., *Ramaswamy et al.*, 2001; *Forster et al.*, 2007, and references therein]. The atmosphere/mixed-layer model studies have suggested that generally the climate sensitivity λ (defined as the ratio of the global near-surface temperature response ΔT per unit radiative forcing ΔF, so $\lambda = \Delta T/\Delta F$) is approximately independent of the forcing mechanism, although λ for strongly absorbing aerosols may differ significantly in some models [e.g., *Hansen et al.*, 1997; *Jacobson*, 2002; *Roberts and Jones*, 2004]. The majority of studies conducted to date have considered the relationship between global radiative forcing and global temperature response. While the radiative forcing from well mixed greenhouse gases such as CO_2 is relatively homogeneous across the globe, the short atmospheric lifetime of aerosol species means that their radiative forcing is highly heterogeneous. Therefore in order to better understand climate change on a more regional scale, the climate response to these more heterogeneous forcing mechanisms needs investigation.

[4] Here, we use an atmosphere/mixed-layer ocean model and apply realistic aerosol and greenhouse gas forcings. We examine the forcing produced by, and the climate response to, changes in three anthropogenic aerosol species: sulfate, biomass-burning and black carbon aerosols, and compare them with the effects of CO_2 increases. The objectives of this study are to investigate:

[5] 1. the climate response to the various forcing agents;

[6] 2. the response of natural primary aerosols (mineral dust and sea-salt);

[7] 3. the relationship between global mean temperature response and global mean forcing;

[8] 4. the additivity of aerosol forcing and response.

2. Experimental Description

[9] The model used in this study is based on the atmospheric component of the HadGEM1 climate model [*Martin et al.*, 2006] coupled to a 50m thermodynamic mixed-layer ocean and sea ice model [*Johns et al.*, 2006]. HadGEM1 includes schemes to simulate sulfate, black carbon and biomass-burning aerosols as fully interactive prognostic

[1]Met Office Hadley Centre, Exeter, UK.

Table 1. Annual-Mean Emissions of Aerosols and Aerosol Precursors for 1860 and 2000

Species	1860	2000
SO_2 + DMS (Tg[S] year^{-1})	33.3	91.2
Biomass-burning (Tg year^{-1})	14.7	37.6
Black carbon (Tg year^{-1})	0.6	7.9

fields, as well as a diagnostic scheme for sea-salt aerosols. Sources of sulfate aerosol include dimethyl sulfide from oceans and SO_2 from volcanic and anthropogenic sources; the latter includes a small contribution (<2% of total S emissions) from biomass burning. Black carbon aerosols are derived from fossil-fuel and biofuel emissions. The black carbon generated by biomass burning is assumed to form an internal mixture with other material generated during burning and forms a generic biomass-burning aerosol.

[10] Various improvements have since been made to these aerosol schemes which significantly improve the simulation of sulfate and biomass-burning aerosols. Additionally, a scheme to simulate mineral dust aerosols based on *Woodward* [2001] has been implemented, and a climatology of biogenic secondary organic aerosols has also been included; all these improvements are detailed by *Bellouin et al.* [2007]. These changes have significantly improved the simulation of aerosols in the model when compared with observations [*Bellouin et al.*, 2007].

[11] The direct effect (scattering and absorption of radiation) of all six aerosol species represented in the model (sulfate, sea-salt, biomass-burning, black carbon, mineral dust and biogenic secondary organic aerosols) is included; the ''semi-direct'' effect of absorbing aerosols (the tendency to reduce cloud by warming due to absorption of radiation; *Hansen et al.*, 1997) is thereby included implicitly. Those aerosols considered to be mainly hydrophilic (sulfate, sea-salt, biomass-burning and the secondary organic aerosols), which therefore act as cloud condensation nuclei (CCN), also contribute to both the first and second indirect effects on clouds [*Twomey*, 1974; *Albrecht*, 1989], treating the aerosols as an external mixture [*Jones et al.*, 2001].

[12] The base configuration of the model uses aerosol emissions and greenhouse gas concentrations representative of the year 1860 (CO_2 concentration of 286.2 ppmv). The effect of anthropogenic sulfate, black carbon and biomass-burning aerosol changes was simulated by changing the emissions of each species in turn to values for the year 2000; for comparison, an experiment was also performed with double the 1860 CO_2 concentration (increased to 572.4 ppmv). Note that this is considerably larger than the 2000 CO_2 concentration of approximately 367 ppmv. The emissions of *Smith et al.* [2004] were used for anthropogenic SO_2, and those of T. Nozawa [2003, personal communication] for black carbon, as in HadGEM1. For biomass-burning aerosols, the emissions specified for the AeroCom project [*Dentener et al.*, 2006] were used, interpolated between the 1750 and 2000 distributions for 1860 according to regional population [*Bellouin et al.*, 2007]. The annual-mean emissions for 1860 and 2000 for the three anthropogenic aerosol species are shown in Table 1.

[13] As we want to include the second indirect effect of those aerosols which act as CCN, we cannot calculate aerosol forcing using the standard method of using two calls to the model's radiation scheme. Instead, we performed ten-year simulations of the model in atmosphere-only mode (i.e., using specified sea-surface temperatures and sea-ice extents) using 2000 emissions, one simulation for each species, and also a control simulation using 1860 emission levels. The difference in the 10-year mean top-of-atmosphere (ToA) net radiation balance compared with the control was taken as a measure of the forcing due to each aerosol. This of course is not an exact forcing but a ''quasi-'' or ''relaxed'' forcing [e.g., *Rotstayn and Penner*, 2001; *Penner et al.*, 2003], and is an approach which captures those processes which have a fast response to the imposed aerosol changes [e.g., *Forster and Taylor*, 2006]. For black carbon aerosol, we also calculate an ''exact'' forcing using the method of a double-call to the radiation scheme; this is because black carbon does not act as a CCN in our model. The difference in the mean forcing between ''quasi'' and ''exact'' methods was not significant at the 5% level. Except where noted, the forcing used for black carbon is the quasi-forcing, for uniformity with the other aerosols.

[14] The forcing due to doubling CO_2 is calculated by calling the model's radiation scheme twice, once with the 1860 concentration and once with the doubled value, and the difference in the radiative flux at the tropopause obtained. Stratospheric adjustment in both the longwave (LW) and shortwave (SW) parts of the spectrum is accounted for when calculating the radiative forcing due to CO_2, but not for the aerosol quasi-forcings, where the effect of stratospheric adjustment is considered small [e.g., *IPCC*, 2007; *Forster et al.*, 2007].

[15] The response to the forcings was determined using the full atmosphere/mixed-layer model. As is usual in such experiments, a preliminary 20-year calibration simulation was performed in order to determine the heat-flux distribution necessary to keep the sea-surface temperatures close to climatological values in the absence of ocean currents, which of course cannot be simulated by a mixed-layer ocean model. This calibration experiment used 1860 anthropogenic aerosol emissions and CO_2 concentrations. The data from the calibration experiment were then used to perform a set of five 30-year simulations with the atmosphere/mixed-layer model:

[16] 1. CTL—aerosol emissions and CO_2 concentration at 1860 levels;

[17] 2. SO4—as CTL, but with anthropogenic sulfate aerosol emissions for 2000;

[18] 3. BB—as CTL, but with biomass-burning aerosol emissions for 2000;

[19] 4. BC—as CTL, but with black carbon emissions for 2000;

[20] 5. CO2—as CTL, but with double the 1860 concentration of CO_2.

[21] The response of the model to the aerosol/CO_2 changes was determined from twenty-year means of each simulation once equilibrium had been reached.

3. Results and Discussion

3.1. Forcing

[22] The distributions of forcing obtained from the atmosphere-only experiments for the 1860–2000 changes in sulfate, biomass-burning and black carbon aerosols, and

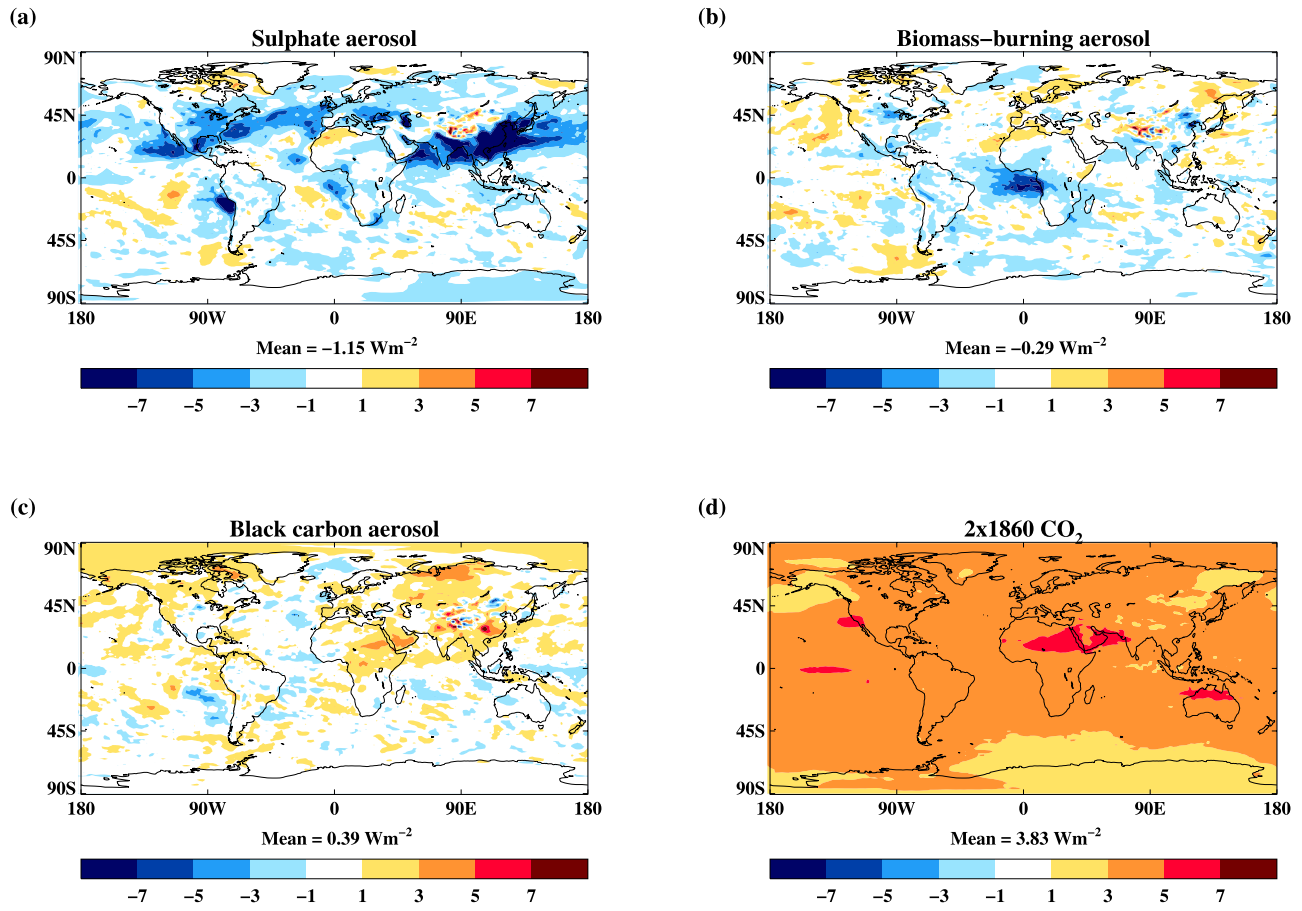

Figure 1. Annual-mean radiative forcing (Wm^{-2}) from the atmosphere-only experiments for each of the forcing agents: (a) for 1860–2000 changes in emissions of anthropogenic sulfate aerosols; (b) As (a) but for biomass-burning aerosols; (c) As (a) but for fossil-fuel black carbon aerosols; (d) For a doubling of 1860 CO_2 concentration.

for a doubling of 1860 CO_2 concentration, are shown in Figure 1. As the global mean values show, there are two species which produce negative (cooling) forcings (sulfate and biomass-burning aerosols) and two which produce positive (warming) forcings (black carbon aerosols and CO_2 increases). The strongest forcing is that due to doubling CO_2 at +3.83 Wm^{-2}, which has a rather uniform, zonally symmetric distribution (Figure 1d). (Note that the forcing for 2000 concentrations of CO_2 would be approximately one third of this.) The next strongest forcing is that due to sulfate aerosol changes at −1.15 Wm^{-2}; although there are some areas of strong forcing in the vicinity of the Peruvian and Namibian stratocumulus decks, the majority of the forcing is concentrated in the northern hemisphere low to midlatitudes (Figure 1a). Next is the forcing from black carbon aerosol at +0.39 Wm^{-2} (Figure 1c). The distribution of forcing by this species is rather diffuse, but definitely asymmetric, with the majority of forcing in the northern hemisphere. Finally, the weakest forcing is due to changes in biomass-burning aerosols (Figure 1b), with a value of −0.29 Wm^{-2}. The forcing by this aerosol is strongly concentrated in the tropical Atlantic, just south of the equator.

3.2. Climate Response

[23] The changes in 1.5 m temperature are shown in Figure 2. The SO4 experiment (Figure 2a) cools globally, but with the most significant cooling in the northern hemisphere. This broadly reflects the distribution of the forcing (Figure 1a), but there is also a strong response over the Arctic where the forcing is minimal. The temperature change in the BB experiment is both smaller and more diffuse in its distribution (Figure 2b), showing changes in both hemispheres in response to a forcing located mainly in the tropics. The temperature change in BC (Figure 2c), although somewhat diffuse, is again strongly asymmetric, with the major warming in the northern hemisphere. As with SO4, there is again a relatively strong temperature response over the Arctic, despite the lack of significant forcing there. Although the global-mean responses in BB and BC are similar in magnitude (but opposite in sign), the geographical distribution of the responses are quite different. Finally, the temperature change due to doubling CO_2 (Figure 2d) shows the classic response of a generally zonal pattern of warming with larger warming at high latitudes. The different patterns of temperature response are emphasized in Figure 3, which shows the zonal mean temperature change normalized by the global-mean forcing for each experiment. The strong response in northern high latitudes

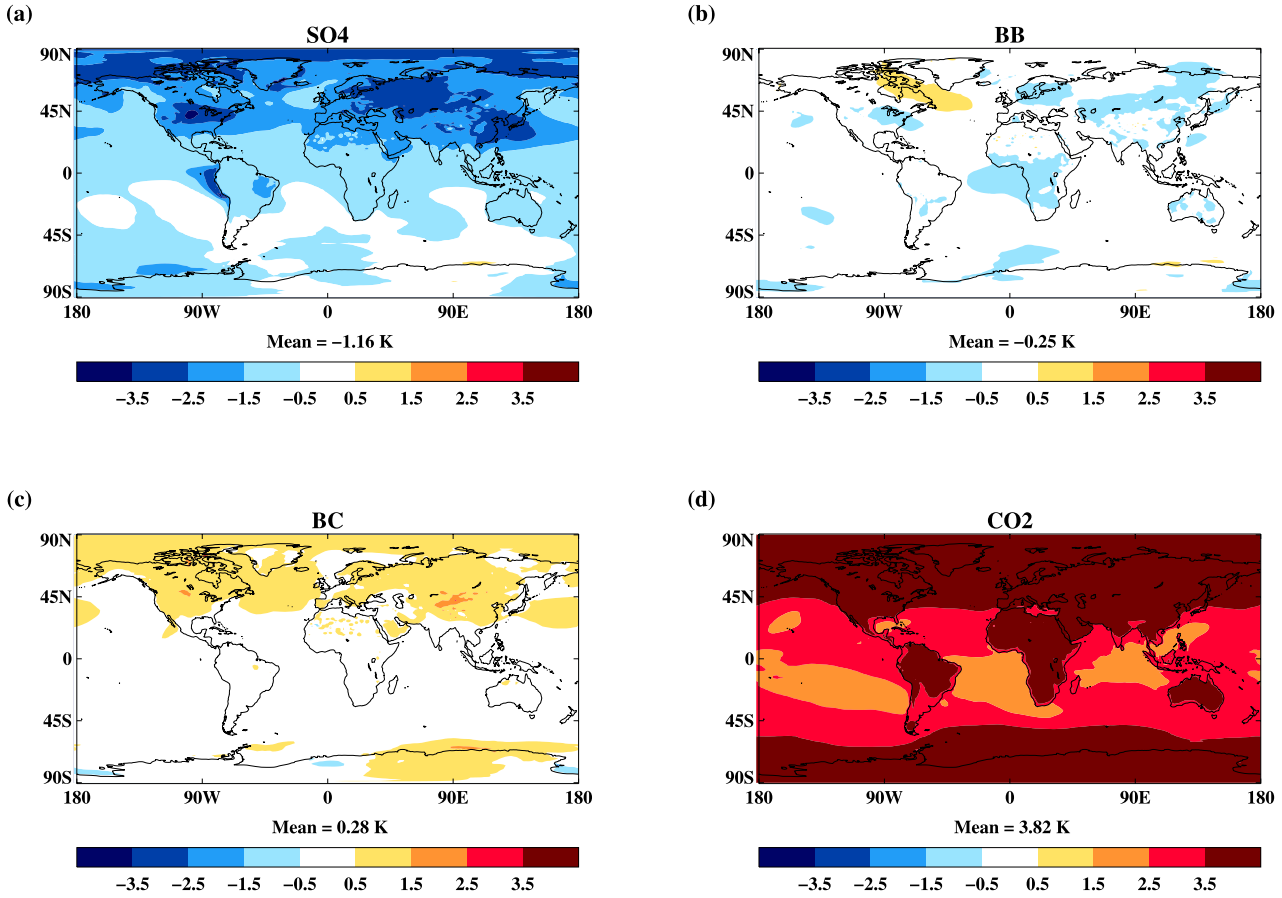

Figure 2. Temperature response at 1.5 m (K) of the atmosphere/mixed-layer model for each experiment with respect to the control simulation CTL: (a) SO4; (b) BB; (c) BC; (d) CO2.

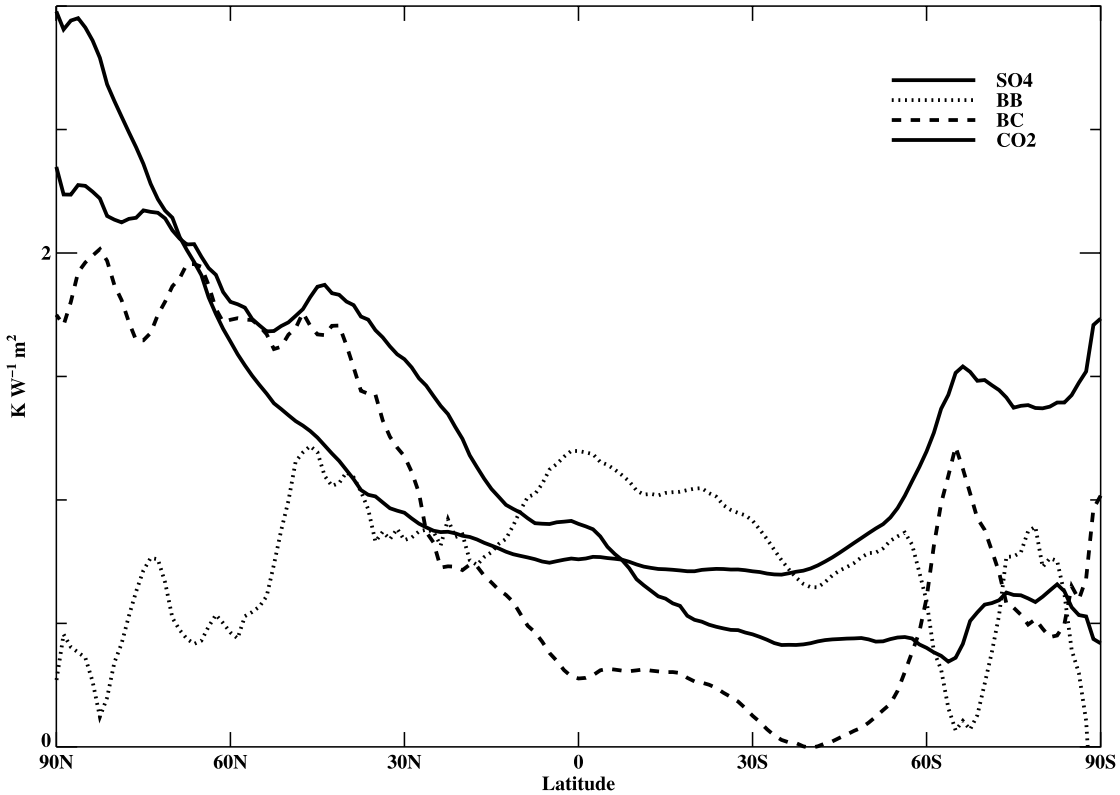

Figure 3. Temperature response normalized by global-mean radiative forcing (K W^{-1} m^2).

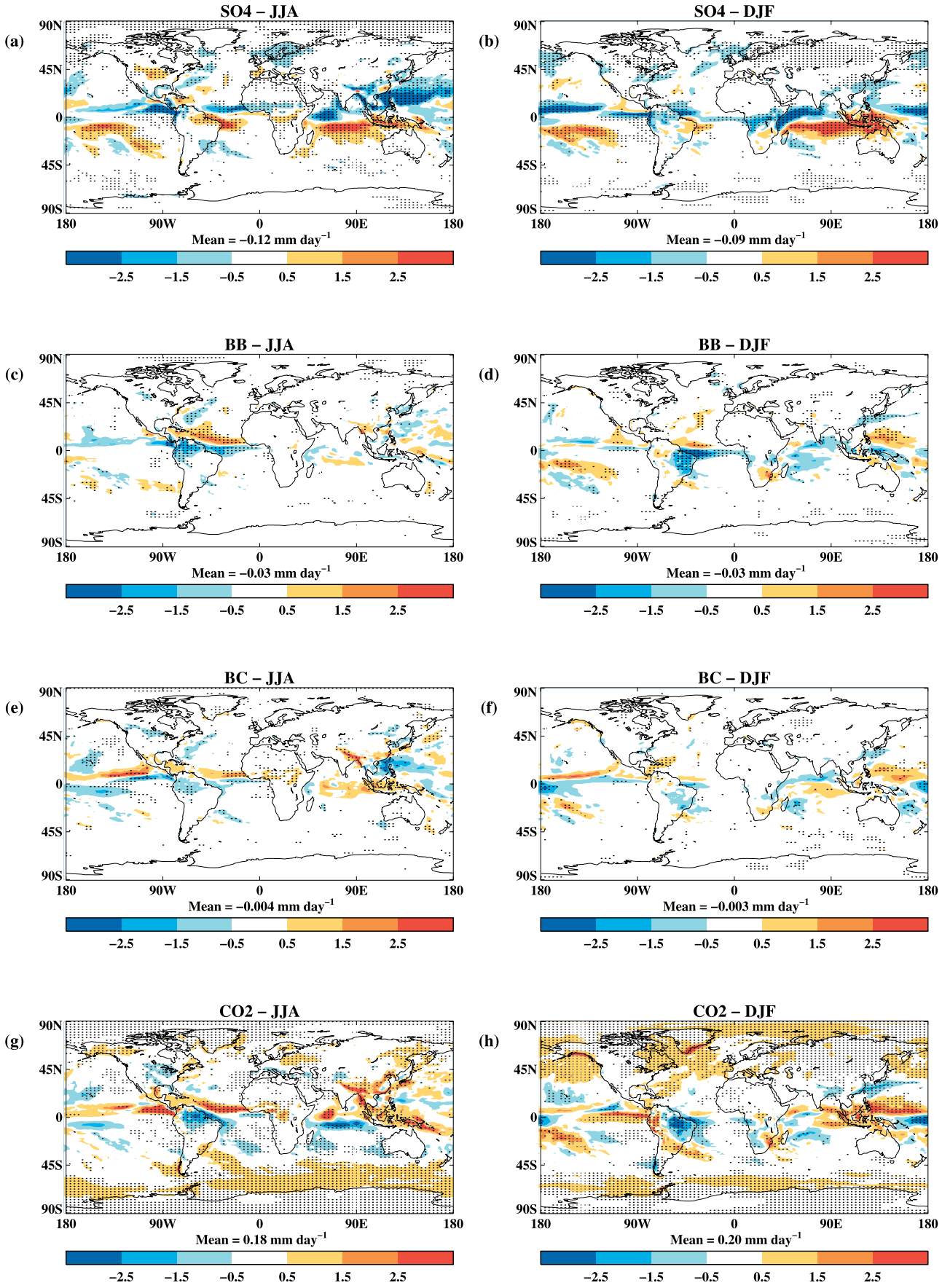
(a)
SO4 – JJA
Mean = −0.12 mm day−1
(b)
SO4 – DJF
Mean = −0.09 mm day−1
(c)
BB – JJA
Mean = −0.03 mm day−1
(d)
BB – DJF
Mean = −0.03 mm day−1
(e)
BC – JJA
Mean = −0.004 mm day−1
(f)
BC – DJF
Mean = −0.003 mm day−1
(g)
CO2 – JJA
Mean = 0.18 mm day−1
(h)
CO2 – DJF
Mean = 0.20 mm day−1
90N
45N
0
45S
90S
180
90W
0
90E
180
−2.5
−1.5
−0.5
0.5
1.5
2.5

Figure 4

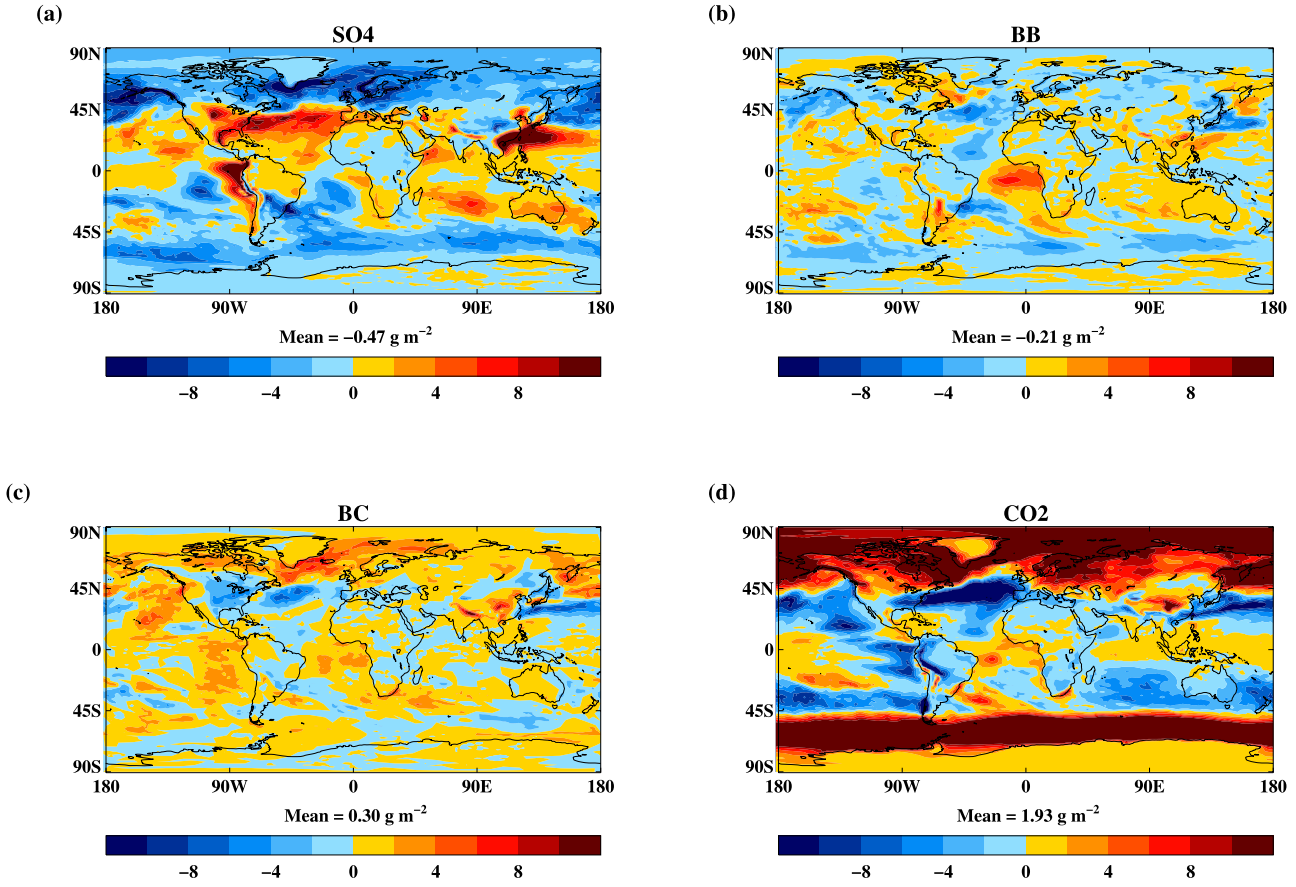

Figure 5. Change in stratiform cloud liquid water path (g m^{-2}) compared with CTL: (a) SO4; (b) BB; (c) BC; (d) CO2.

in SO4 and BC is quite different to the response in BB, which is more symmetric with a slight maximum in the tropics. The response in CO2 is amplified toward both poles, but is higher in the Arctic.

[24] The impact of the various forcings on precipitation is shown in Figure 4 which shows the change in mean June–August and December–February precipitation distributions with respect to CTL. The response is not a simple function of the global temperature change: two models cool (SO4 and BB) and two warm (BC and CO2), yet in three simulations (BB, BC and CO2) the ITCZ moves northward. As noted by previous studies [*Williams et al.*, 2001; *Rotstayn and Lohmann*, 2002; *Roberts and Jones*, 2004; *Biasutti and Giannini*, 2006], it is the inter-hemispheric balance of the temperature change which is important: those simulations which have strongly asymmetric forcings (SO4 and BC) show the ITCZ moving in opposite directions, southwards in SO4 (cooler northern hemisphere) and northward in BC (warmer northern hemisphere). The same principle applies to BB and CO2: the fact that the (cooling) forcing is located to the south of the equator in BB (Figure 1b) contributes to the northward migration of the ITCZ. Note that the forcing due to biomass-burning aerosols, the most localized of the four, produces its most significant precipitation changes in the Atlantic, whereas the others produce changes throughout the tropics and subtropics. The less asymmetric warming in CO2 is still sufficient for the ITCZ to move northward in a similar fashion to that observed in BC, despite the forcing distributions being quite different. There are also interesting regional differences in the changes in precipitation, especially in semi-arid regions: e.g., whereas the southward migration of the ITCZ in SO4 reduces precipitation in the Sahel region of Africa in July–August, it increases in the Nordeste region of Brazil. The opposite is true in BB, BC and CO2.

[25] The change in stratiform-cloud liquid water path (vertically integrated cloud liquid water content; LWP) is shown in Figure 5. These changes are interesting when considered in light of the second indirect aerosol effect: in the model, increasing numbers of CCN tend to increase cloud LWP for a given amount of rainfall, i.e., increasing CCN decreases precipitation efficiency. Both sulfate and biomass-burning aerosols act as CCN in the model, whereas black carbon aerosols do not, and of course CO_2 concentrations have no direct impact on cloud microphysics. One might therefore expect to see increases in LWP in the SO4

Figure 4. Change in mean June–August (left column) and December–February (right column) precipitation rate (mm day^{-1}) compared with CTL: (a) and (b) SO4; (c) and (d) BB; (e) and (f) BC; (g) and (h) CO2. Dots indicate changes which are significant at the 5% level.

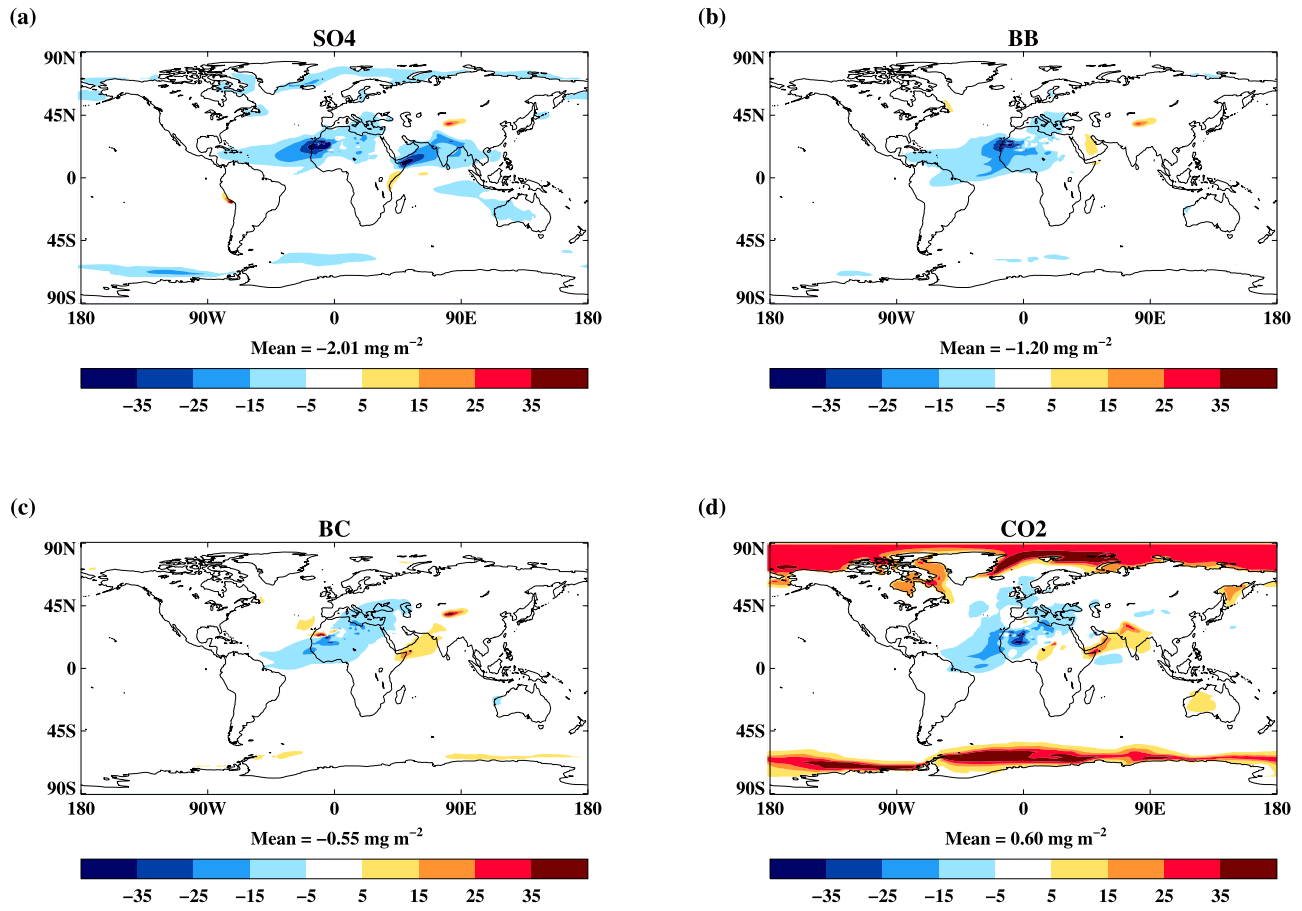

Figure 6. Change in natural primary aerosol burden (mg m^{-2}) compared with CTL: (a) SO4; (b) BB; (c) BC; (d) CO2. The changes at high latitudes are caused by sea-salt, those at low latitudes by mineral dust aerosols.

and BB experiments, but in fact the reverse is true in the global mean. In fact, the change in LWP appears to be dominated by large-scale atmospheric responses. At high latitudes, the LWP changes are due to responses in the mixed-phase cloud region: the ice/water balance shifts toward the ice phase in those experiments which cool and toward the liquid phase in those which warm [*Senior and Mitchell*, 1993]. The complex response in the tropics and midlatitudes is related to poorly understood low-cloud feedback processes which are the subject of ongoing research. In general, the LWP response is more dependent on thermodynamic than on microphysical processes.

3.3. Response of Natural Primary Aerosols

[26] Figure 6 shows the change in the burden of the natural primary aerosols (sea-salt and mineral dust) in the four experiments SO4, BB, BC and CO2 with respect to the control simulation CTL. These changes are purely in response to the anthropogenic aerosol/CO_2 changes, as no alterations to the emission schemes for natural aerosols were made in these experiments (vegetation cover was also kept constant). The changes at low latitudes are dominated by mineral dust, while those at high latitudes are due to sea-salt. The changes in dust burden show complex patterns of increases and decreases, with some areas of increase immediately adjacent to areas of decrease e.g., the Western Sahara in BC and further east in CO2. Such complex distributions of changes are to be expected given the highly variable nature of dust emission [*Woodward*, 2001]: whereas one might explain the changes in the dust plume over the Arabian Sea in terms of the change in wind speed over the horn of Africa (see Figure 9), the same explanation does not hold for the plume extending over the Atlantic. We concentrate on the area between 0°–40°N and 20°W–90°E, the main area of dust production in global terms. Figure 7 shows the correlation between the changes in dust emission and soil moisture content in this region, and Figure 8 shows a similar plot against the change in 10m wind speed. Points with negligible emission changes ($<1 \times 10^{-10}$ kg m^{-2} s^{-1}, i.e., 0.0086 g m^{-2} day^{-1}) are not included in these plots. This neglects 90% of the land points within the region, but such points in fact have essentially no dust production, due to the various threshold terms in the dust generation scheme. These results indicate that changes in dust production in this major source region are in general more strongly affected by changes in soil moisture content than in wind speed in this model.

[27] Turning to the changes in sea-salt, these appear more straightforwardly related to changes in sea-ice fraction (Table 2) and 10 m wind speed (Figure 9), which govern the area available for sea-salt production and the amount of sea-salt produced respectively. Experiment SO4 has

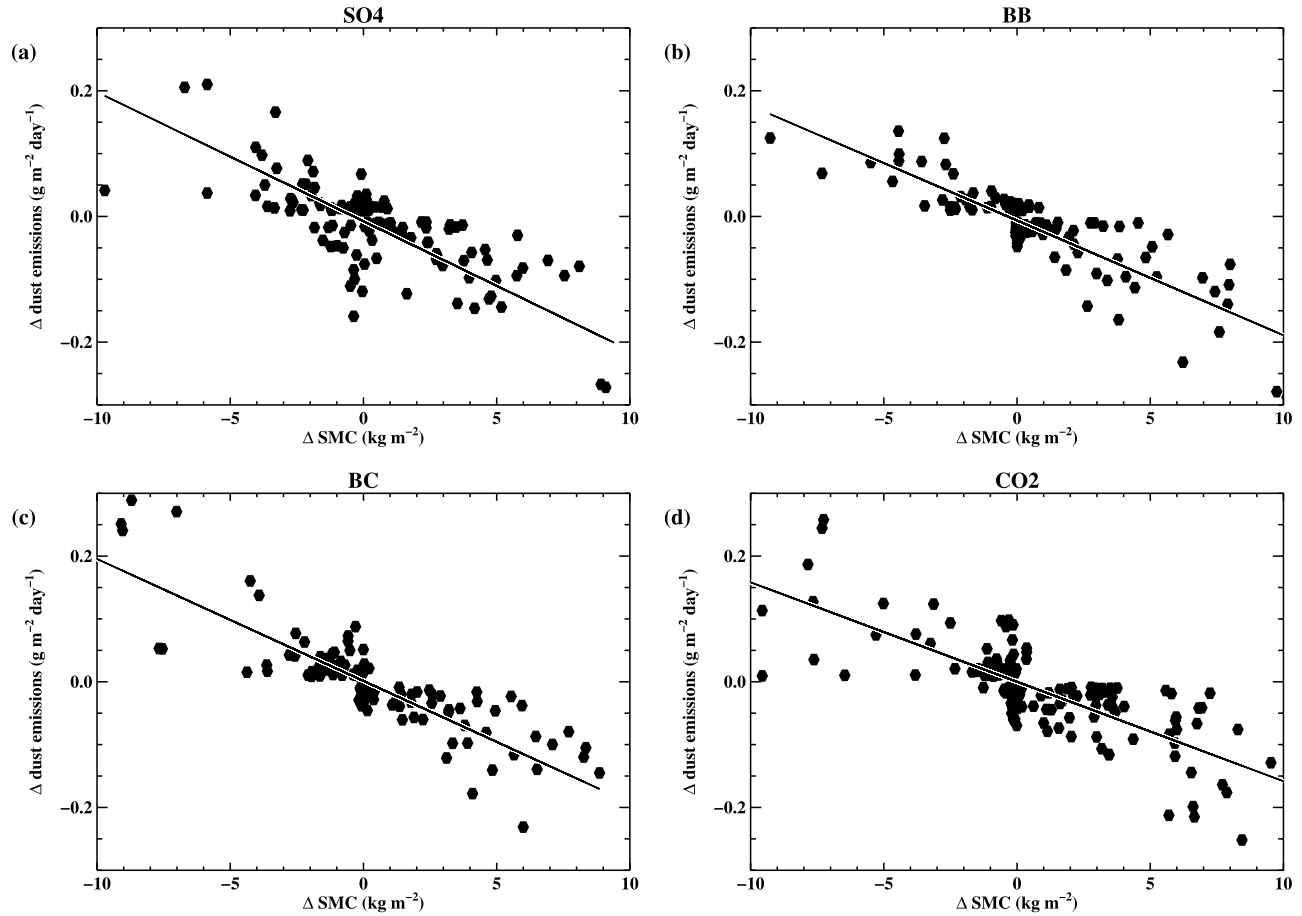

Figure 7. Scatterplot of the change in mineral dust emission (g m^{-2} day^{-1}) against the change in soil moisture content (kg m^{-2}) compared with CTL for land points in the region 0°–40°N and 20°W–90°E, with the best fit straight line; see text for more details. (a) SO4; (b) BB; (c) BC; (d) CO2.

increases in sea-ice at both poles, but with a larger change in the northern hemisphere; the increases in BB are much smaller (Table 2). This reflects the differing amount of high-latitude temperature change in each experiment. These changes in sea-ice, and the corresponding decreases in wind speed (possibly related to the increased roughness length over sea-ice), lead to a reduction in sea-salt around the sea-ice edges in these experiments (Figures 6a and 6b). The BC experiment has a only a small tendency in the opposite direction, whereas in CO2 there is a much larger reduction in sea-ice in both hemispheres. This, along with corresponding wind speed increases, causes sizable sea-salt increases in these areas in CO2 (75% and 51% increases in sea-salt burdens poleward 60°N and 60°S respectively).

3.4. Climate Sensitivity

[28] Using the global mean forcing from the atmosphere-only experiments and the near-surface temperature change from the atmosphere/mixed-layer simulations, values of climate sensitivity (degrees K of temperature change per Wm^{-2} of forcing) for each type of forcing can be computed; the results are given in Table 3.

[29] The climate sensitivities to sulfate aerosol (λ_{SO4}) and CO_2 (λ_{CO2}) are essentially identical, confirming the result of *Williams et al.* [2001]. This is despite the fact that Williams et al. used a previous generation of the Hadley Centre model which had a lower climate sensitivity (0.85 K W^{-1}m^2) and considered only the indirect effects of sulfate aerosol. However, the sensitivity to the three aerosol species is not the same: the climate sensitivity for black carbon (λ_{BC}) appears markedly lower than that due to the other forcing agents. However, as can be seen from Table 3, the 95% confidence interval for λ_{BC} is wide, and a test shows that it is not significantly different to λ_{CO2} at the 5% level. The main reason for this is the low signal-to-noise ratio of the black carbon quasi-forcing; the atmosphere-only simulations used to determine the forcing would need to be many times longer to avoid this. We therefore also calculated black carbon climate sensitivity using the "exact" rather than the quasi-forcing (λ^*_{BC}). This yielded a value of 0.62 K W^{-1}m^2, with a much reduced 95% confidence interval of 0.50–0.74 K W^{-1}m^2; this is because of the improved signal-to-noise ratio of the exact forcing (0.45 ± 0.01 Wm^{-2}). The difference between λ^*_{BC} and λ_{CO2} is significant at the 5% level, and we therefore have confidence that it is worth investigating the response to black carbon further (see below).

[30] The lower value of climate sensitivity to black carbon compared with that to CO_2 is in agreement with the findings of *Roberts and Jones* [2004]. They found that climate sensitivity to black carbon was about 62% of that to CO_2 (i.e., black carbon had a climate efficacy of 62%) in

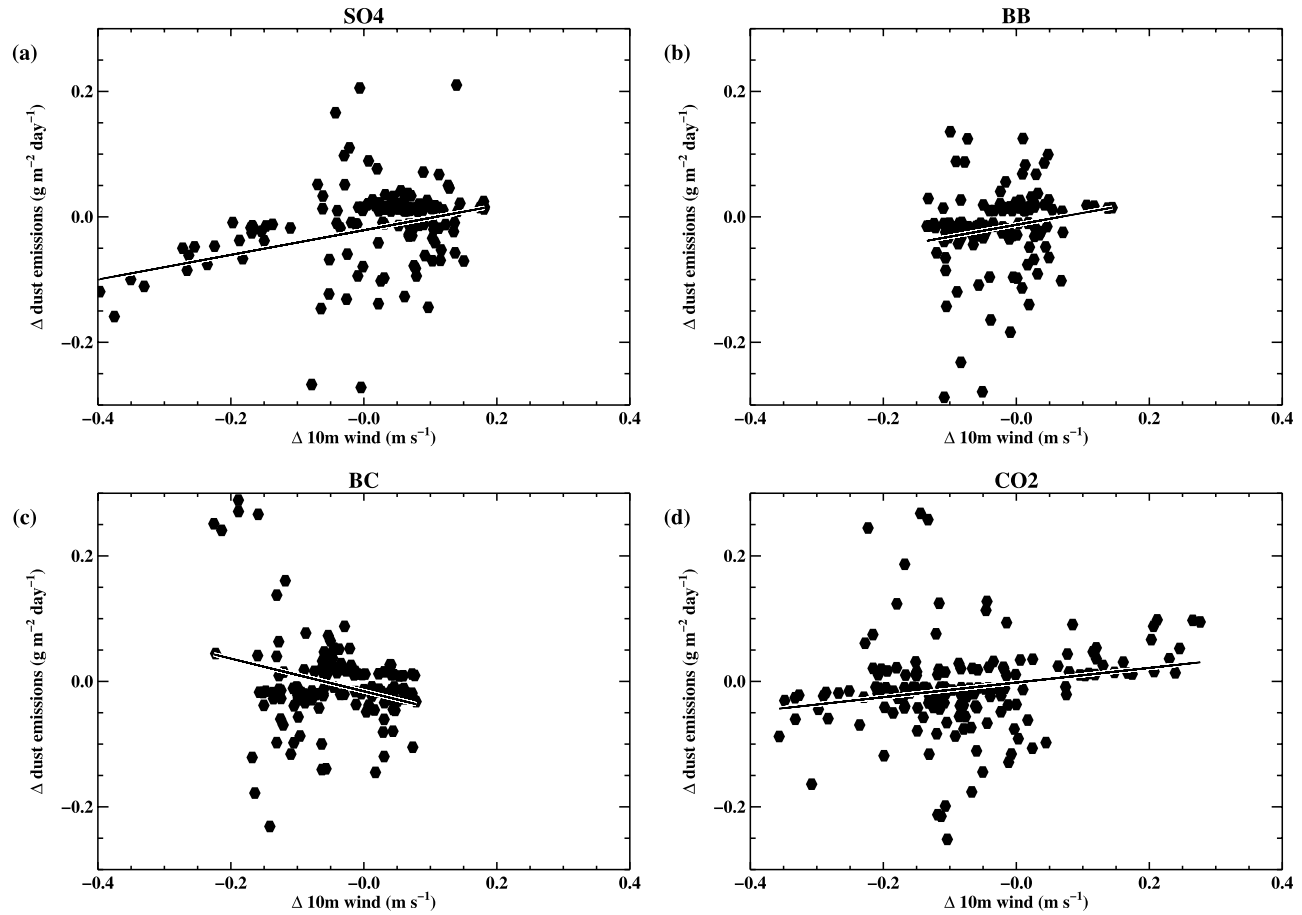

Figure 8. As Figure 7 but as a function of the change in 10 m wind speed (m s^{-1}): (a) SO4; (b) BB; (c) BC; (d) CO2.

their model, the same as that used by Williams et al. The present study indicates a climate efficacy of 71% for black carbon if using the quasi-forcing, or 62% [as in *Roberts and Jones*, 2004] if using the the exact forcing. Reduced efficacy for black carbon aerosol has also been found in studies with other models: *Hansen et al.* [2005] and *Lohmann and Feichter* [2005] found efficacies very similar to the present study. On the other hand, a recent study by *Sokolov* [2006] found a higher efficacy for black carbon than for CO_2. No consensus has yet emerged regarding the efficacy of black carbon aerosols [*Forster et al.*, 2007].

[31] In order to investigate the reason why black carbon has a lower climate sensitivity than the other forcing agents in our model, it is useful to be able to directly compare the responses due to the various forcings. To this end we normalize the various responses by the global annual mean forcing for each species given in Table 3 (i.e., the quasi-forcing is used for all aerosols, for uniformity); the results are presented in Table 4. It must therefore be borne in mind that the forcing from sulfate and biomass-burning aerosols is of opposite sign to that from black carbon and CO_2 when considering the results given in Table 4.

[32] The normalized change in sea-ice area is similar for sulfate and black carbon aerosols at -2.8 and -3.1×10^6 km^2 W^{-1} m^2 respectively (indicating an increase in sea-ice for sulfate and a decrease for black carbon, as the normalizing forcings are of opposite sign). This is related to the fact that the forcings from both species are largely confined to the northern hemisphere, and are significant at high latitudes (Figure 1). A doubling of CO_2,which produces a temperature change response showing the greatest high-latitude amplification (Figure 3), has the highest sea-ice feedback at -4.5×10^6 km^2 W^{-1} m^2.The weakest feedback on sea-ice, at -1.0×10^6 km^2 W^{-1} m^2, is due to the biomass-burning aerosols, apparently because the forcing by this species is largely localized to the tropical Atlantic. It therefore seems clear that a difference in the strength of the sea-ice feedback is not a cause of the lower value of λ_{BC}.

[33] The normalized change in vertically integrated water vapor shows the first sign of anomalous behavior in the case of black carbon. This quantity is remarkably similar for sulfate, biomass-burning and CO_2, with a range of only 1.54 to 1.56 kg m^{-2} W^{-1} m^2, whereas the value for black carbon

Table 2. Changes in Sea-Ice Area ($\times 10^6$ km^2) in the Northern (NH) and Southern (SH) Hemispheres in the Four Experiments

Experiment	NH	SH
SO4	+2.26	+0.93
BB	+0.05	+0.23
BC	−0.73	−0.50
CO2	−10.32	−7.05

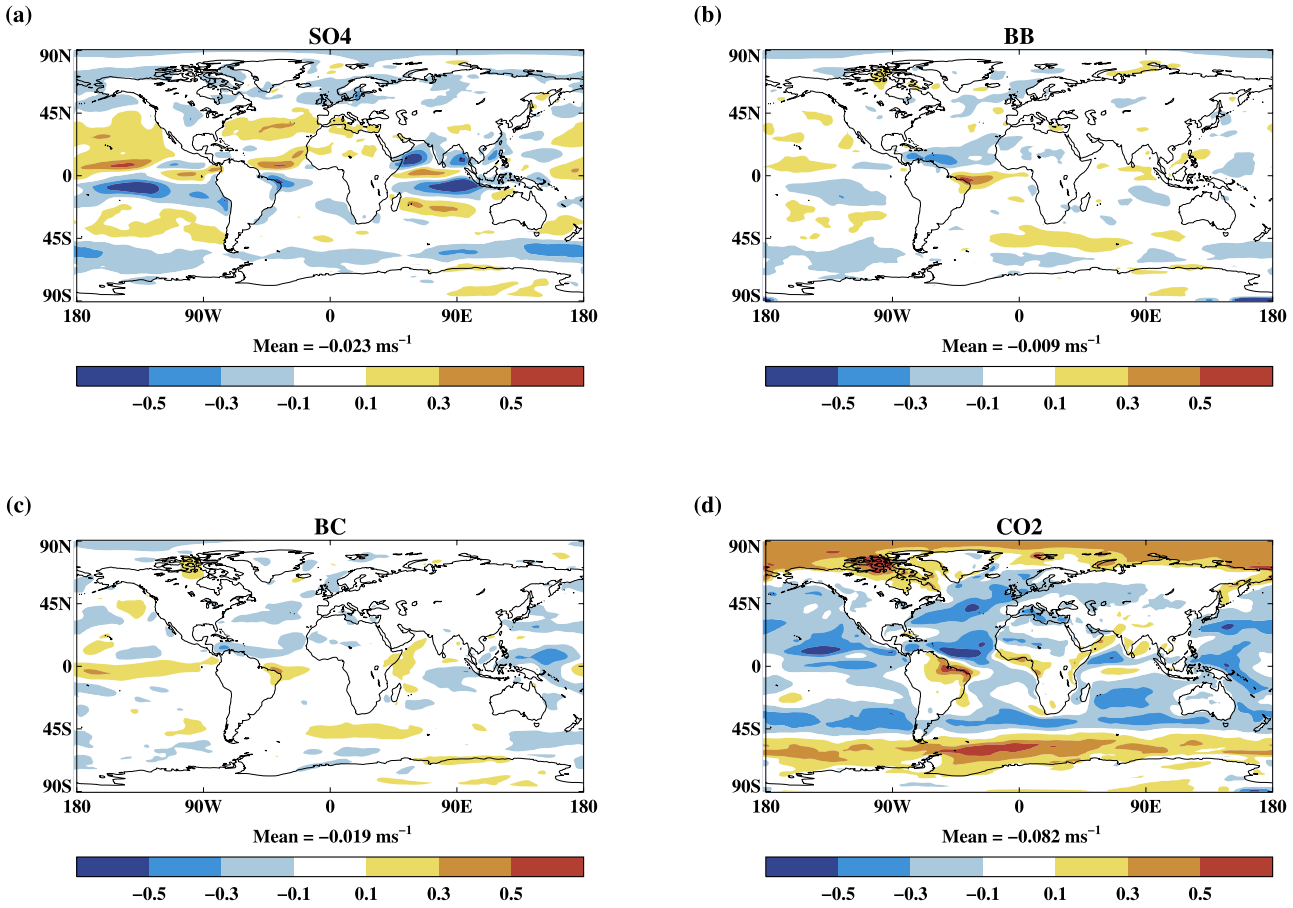

Figure 9. Change in 10 m wind speed (m s^{-1}) compared with CTL: (a) SO4; (b) BB; (c) BC; (d) CO2.

is approximately 25% less at 1.14 kg m^{-2} W^{-1} m^2. As vertically integrated water vapor tends to be dominated by the boundary layer, it is useful to also examine the vertical profile of forcing-normalized water vapor changes, as shown in Figure 10. In all cases, the change in the upper troposphere (above about 500 mb) acts to reinforce the respective forcings, i.e., reductions in SO4 and BB and increases in BC and CO2 (recall the difference in sign of the forcings). As with SO4, the change in BC is mostly concentrated in the northern hemisphere, but also includes a small change in the opposite sense in the upper troposphere south of the equator. These results suggest that the water vapor feedback operates somewhat differently for black carbon compared with the other forcing agents, acting to reduce λ_{BC}.

[34] The normalized change in cloud forcing also shows anomalous behavior for black carbon. As with upper-tropospheric water vapor, cloud forcing changes due to sulfate, biomass-burning and CO_2 act to reinforce the forcing due to each species (Table 4). Sulfate causes shortwave cloud forcing (SWCF) to become increasingly negative and also decreases the positive longwave cloud forcing (LWCF) slightly. Biomass-burning aerosols have an almost equal impact on both SWCF and LWCF, both acting in the direction of further cooling. CO_2 has only a slight impact on cloud forcing in both parts of the spectrum, but such as it is, it enhances the warming. Black carbon has a similar impact to CO_2 on SWCF, but the net effect is dominated by the change to LWCF, which, unlike CO_2, is such as to decrease the warming effect of the LWCF. The net impact is that sulfate, biomass-burning and CO_2 all invoke cloud feedbacks which enhance the applied forcing, whereas the cloud feedback for black carbon counteracts the initial forcing. This can be seen in Figure 11, which compares the changes in forcing-normalized total cloud condensed water content. The decrease in condensed water content at northern midlatitudes in the black carbon case (Figure 11c), perhaps due to the semi-direct effect, is clear. The changes at upper levels are due to a reduction in cloud

Table 3. Global Annual-Mean Forcing (ΔF, ± One Standard Deviation), Near-Surface Temperature Change (ΔT, ± One Standard Deviation), Climate Sensitivity (λ, With 95% Confidence Interval) and Climate Efficacy for 1860–2000 Changes in Sulfate, Biomass-Burning and Black Carbon Aerosols, and a Doubling of 1860 CO_2 Concentration

Species	ΔF (Wm^{-2})	ΔT (K)	λ(K W^{-1} m^2)	Efficacy (%)
Sulfate	−1.15 ± 0.06	−1.16 ± 0.02	1.01 (0.89–1.16)	101.2
Biomass-burning	−0.29 ± 0.07	−0.25 ± 0.03	0.86 (0.51–2.09)	86.7
Black carbon	+0.39 ± 0.09	+0.28 ± 0.03	0.71 (0.44–1.51)	71.2
CO_2	+3.83 ± 0.06	+3.82 ± 0.04	1.00 (0.85–1.14)	100.0

Table 4. Global Annual-Mean Responses, Normalized by the Global Annual-Mean Forcing, for 1860–2000 Changes in Sulfate, Biomass-Burning and Black Carbon Aerosols, and a Doubling of 1860 CO_2 Concentration[a]

Normalized Response	SO4	BB	BC	CO2
Sea-ice area (10^6 km^2/Wm^{-2})	−2.77	−0.99	−3.12	−4.53
Column water vapor (kg m^{-2}/Wm^{-2})	+1.56	+1.54	+1.14	+1.54
Shortwave cloud forcing (Wm^{-2}/Wm^{-2})	+0.78	+0.28	+0.05	+0.05
Longwave cloud forcing (Wm^{-2}/Wm^{-2})	+0.08	+0.27	−0.26	+0.04
Net cloud forcing (Wm^{-2}/Wm^{-2})	+0.86	+0.55	−0.21	+0.08
Surface net radiation (Wm^{-2}/Wm^{-2})	+1.89	+2.55	−0.77	+1.08
Precipitation rate (mm day^{-1}/Wm^{-2})	$+7.7 \times 10^{-2}$	$+8.5 \times 10^{-2}$	-5.4×10^{-3}	$+5.0 \times 10^{-2}$

[a]Quantities which are strictly dimensionless (e.g., normalized cloud forcing) are still given units of Wm^{-2}/Wm^{-2} to emphasize the uniform approach.

ice content, and such high-level clouds are those of importance for LWCF.

[35] The fact that black carbon is a much more absorbing aerosol than either sulfate or biomass-burning aerosols will clearly have an impact on the surface radiation balance. Table 4 shows that the forcing-normalized change in surface net radiation is again in the opposite sense for black carbon compared with the other species. Indeed, this is the main difference between black carbon and the other forcing agents. For the latter, the physical processes involved mean that the ToA forcing is of the same sign as the surface forcing. Sulfate and biomass-burning aerosols cause increases in reflected ToA SW radiation and corresponding decreases in surface SW. Surface SW is reduced in CO2 (which opposes the positive ToA forcing), but this is more than compensated for by an increase in downwelling LW, again leading to surface forcing of the same sign as that at ToA. As it has little significant effect in the LW, black carbon has no such counterbalancing LW effect, and leads to a surface forcing of opposite sign to that at ToA. It should be noted, however, that unlike some other models [e.g., *Jacobson*, 2004], the model used here does not currently include a treatment of the impact of deposited black carbon on the albedo of lying snow. The inclusion of such an effect

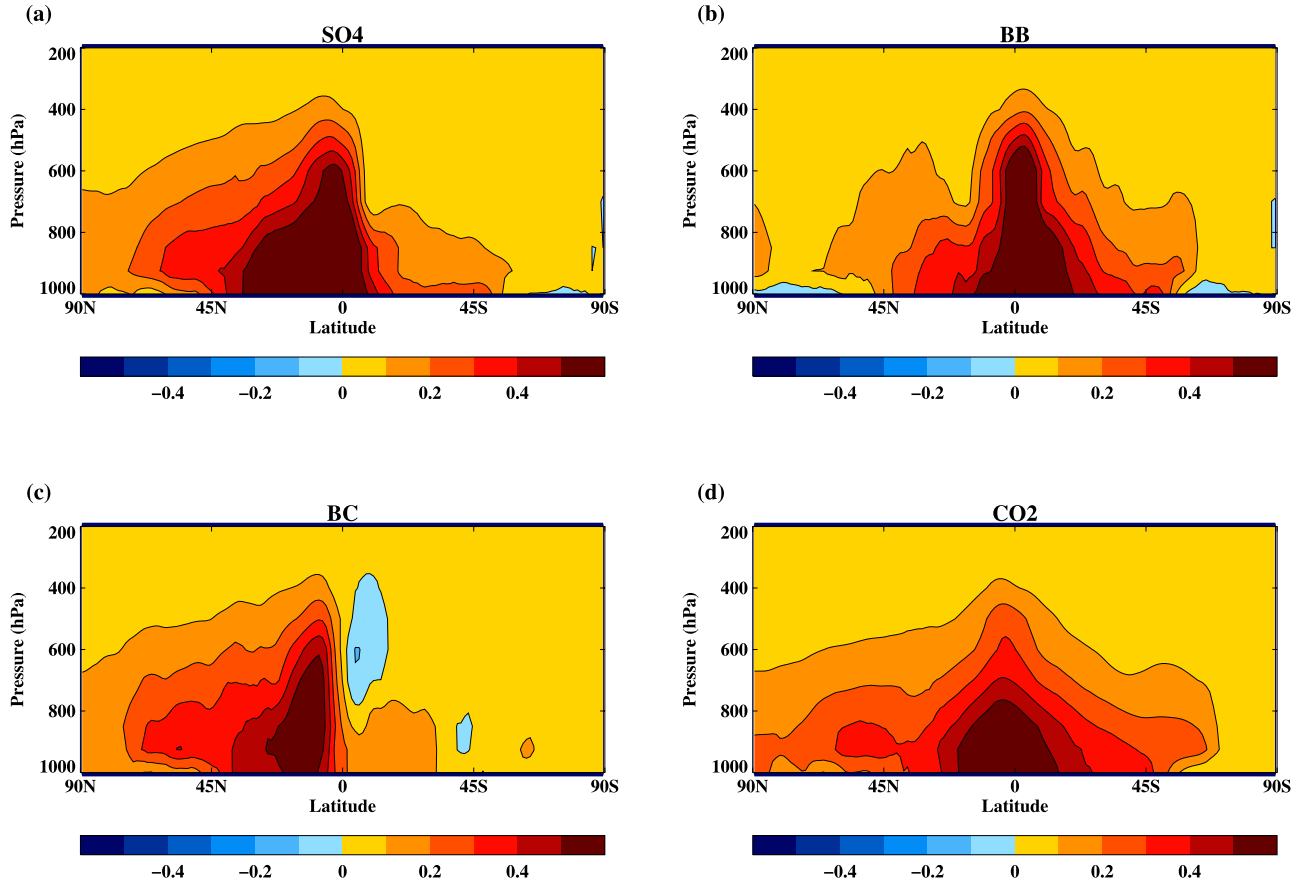

Figure 10. Change in tropospheric water vapor mass mixing ratio compared with CTL normalized by global annual mean radiative forcing for each experiment (g kg^{-1} W^{-1} m^2): (a) SO4; (b) BB; (c) BC; (d) CO2.

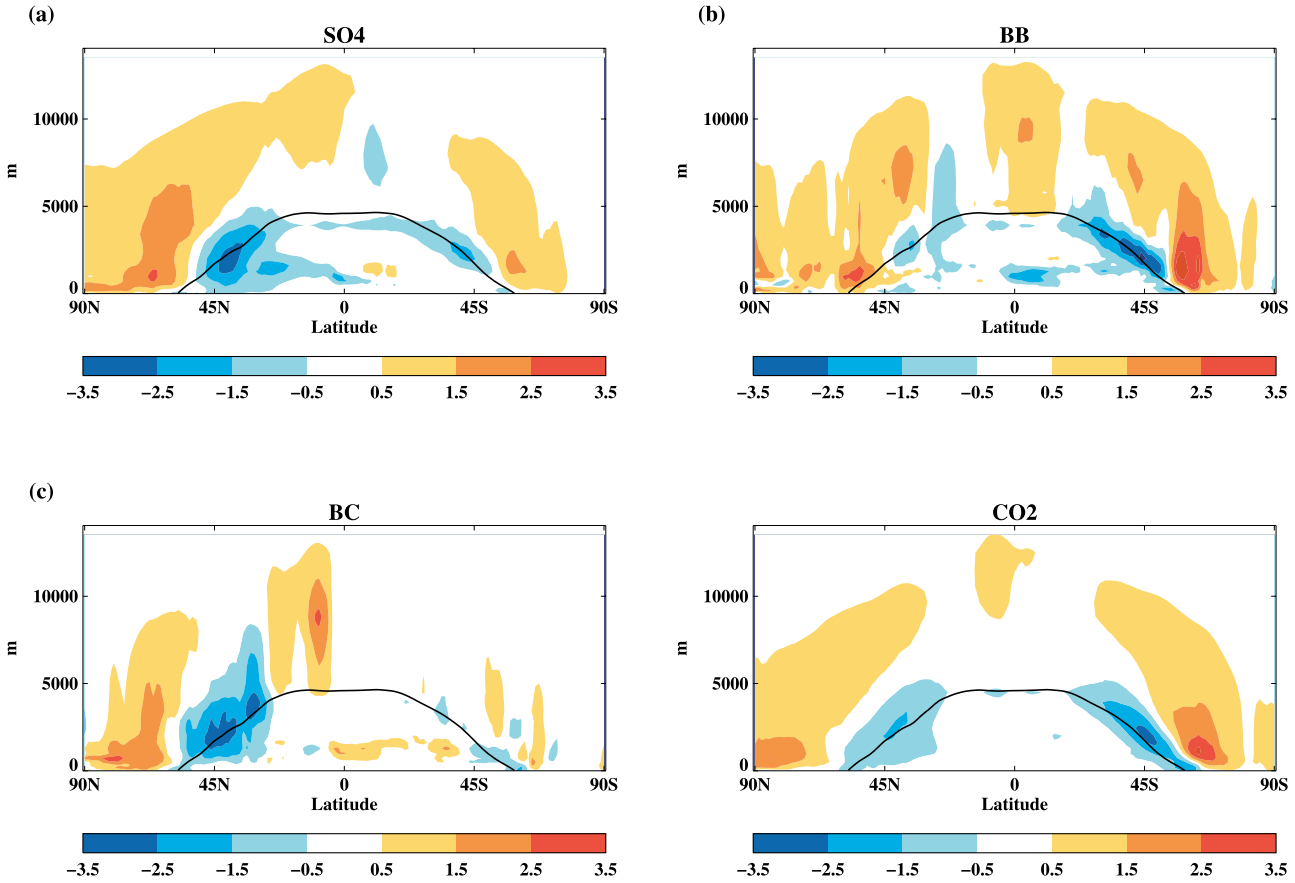

Figure 11. Change in stratiform cloud total condensed water content compared with CTL normalized by global annual mean radiative forcing for each experiment (mg kg^{-1} W^{-1} m^2): (a) SO4; (b) BB; (c) BC; (d) CO2. The 0°C isotherm from CTL is overlaid.

could increase the impact of black carbon on the surface energy balance, possibly increasing λ_{BC}.

[36] The impact of the changes in surface net radiation can be seen in the forcing-normalized change in global-mean precipitation rate (Table 4). All three aerosol species show a decrease, illustrating that the change in precipitation does not depend simply on whether a forcing is positive (CO_2 and black carbon) or negative (sulfate and biomass-burning aerosols).

3.5. Additivity of Forcing and Response

[37] A further pair of experiments were also performed to assess to what degree the forcing by and response to anthropogenic aerosol changes were additive. The atmosphere-only simulations to determine the forcing, and the atmosphere/mixed-layer simulations for the response (experiment "ALL"), were conducted in the same manner as those for the other aerosols, except that all three anthropogenic aerosol emissions were increased to their 2000 levels simultaneously.

[38] The global annual-mean forcing due to all anthropogenic aerosols is -1.18 ± 0.09 Wm^{-2}, which is in reasonable agreement with the sum of the forcings due to sulfate, biomass-burning and black carbon aerosols considered separately, -1.05 ± 0.13 Wm^{-2}. The zonal-mean distribution of the forcings are shown in Figure 12a; apart from the high southern latitudes, the sum of the individual forcings (red line) follows closely that determined from a simultaneous change in all anthropogenic aerosols (black line), the latter appearing as a smoothed version of the former. The sum of the changes in near-surface temperature is -1.13 ± 0.04 K, which is similar to the change of -1.07 ± 0.03 K in experiment ALL (although the values do differ at the 5% significance level). As shown in Figure 12b, the distribution of the temperature change in ALL (black line) again appears as a somewhat smoothed version of the sum of the individual changes (red line), as with the forcings. The climate sensitivity from experiment ALL is 0.90 K W^{-1} m^2.This is somewhat less than that determined using the sum of the individual aerosol forcings and responses, 1.08 K W^{-1} m^2, mainly due to the less precise additivity of the forcings.

[39] Figure 12c shows a comparison of the changes in annual-mean precipitation rate; the correspondence of the two is remarkably close when the different responses for the individual aerosol species is considered (Figure 4). Such additivity is not found for all quantities, however: the change in the natural primary aerosol burden in ALL (-1.23 ± 0.38 mg m^{-2}) is significantly different (at the 5% level) to the sum of the responses from SO4, BB and BC (-3.75 ± 0.77 mg m^{-2}). Figure 12d shows the zonal-mean of the responses; although the structure of both responses is similar, that from ALL is of much lower

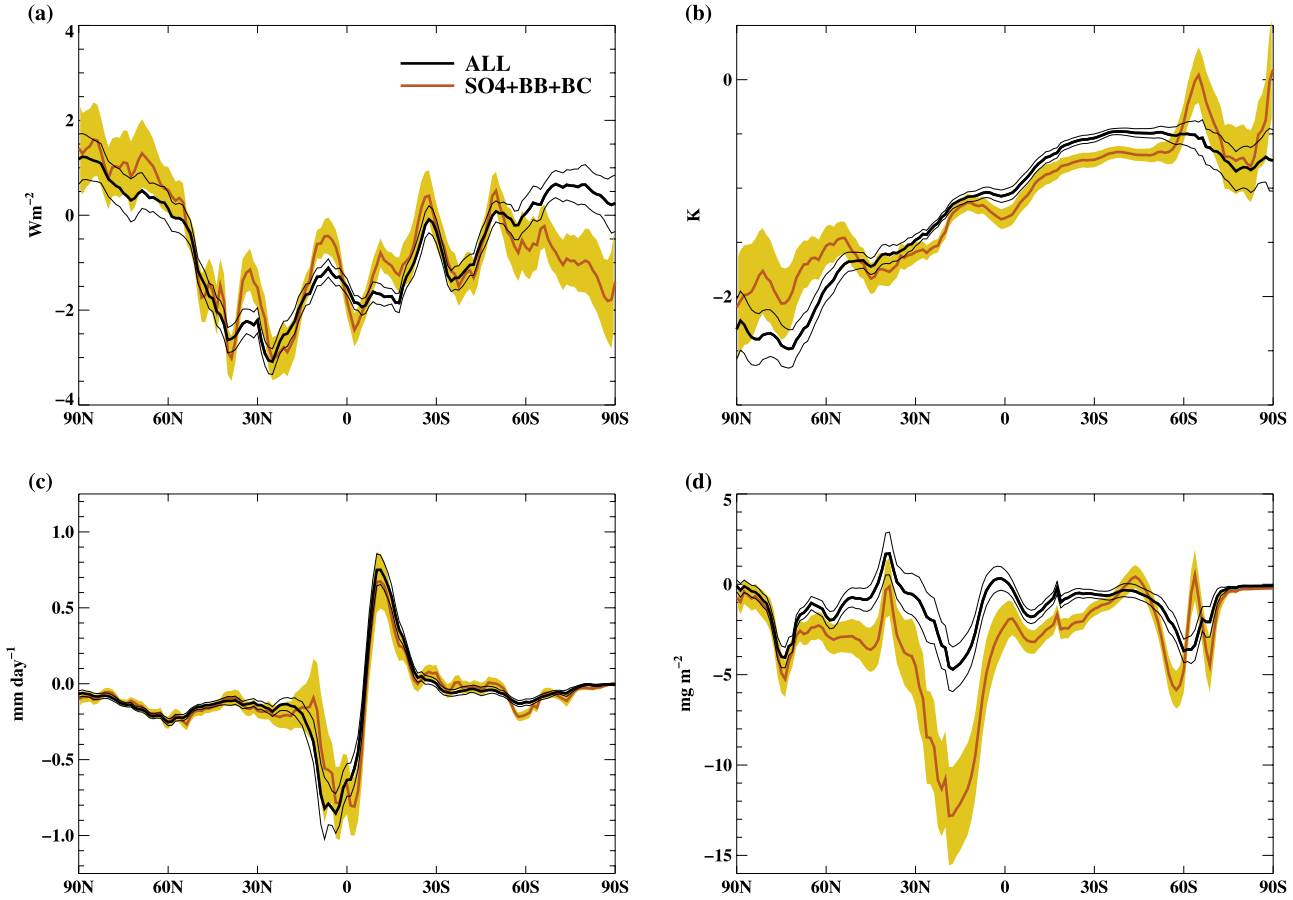

Figure 12. The effects of changing all aerosols simultaneously compared with the sum of changing them individually. The thick black line represents the mean of the simultaneous changes, with one standard deviation indicated by the thin lines. The red line shows the mean impact of the sum of the individual changes, with one standard deviation indicated by the yellow shading. (a) Radiative forcing (Wm^{-2}); (b) Change in 1.5 m temperature (K); (c) Change in annual-mean precipitation rate (mm day^{-1}); (d) Change in natural primary aerosol burden (mg m^{-2}).

amplitude. The location of the greatest discrepancy indicates that it is a difference in the response of Saharan mineral dust, a highly variable quantity, which is mainly responsible.

[40] These results are similar to those of *Ramaswamy and Chen* [1997] with a low-resolution atmosphere/mixed-layer model with fixed cloud microphysical properties and amounts, and also of *Haywood et al.* [1997] who performed a similar study using a fully coupled atmosphere-ocean GCM. Both found that the effects of albedo perturbations and CO_2 forcing added reasonably linearly. This result was also found by *Gillett et al.* [2004] using a very early version of the Hadley Centre model (HadCM2) of much lower resolution and including only a simple parameterization of only the direct effect of sulfate aerosol. *Sexton et al.* [2003], on the other hand, did find some evidence of non-linear interaction between greenhouse gases and forcing from the first indirect effect of sulfate aerosol in the HadCM3 model. However, the parameterization of this aerosol effect is very simple in their model, and is not interactive. Our study, with increased model resolution and more physical parameterization of aerosol effects, suggests that linear additivity does still apply, if only for the aerosol forcings studied here. The additivity of global-mean temperature response from various forcing mechanisms for other non-Met Office model studies is discussed in detail by *Forster et al.* [2007].

4. Conclusions

[41] We have used an atmosphere/mixed-layer ocean version of the Hadley Centre climate model to investigate the forcing by, and climate response to, changes in three different anthropogenic aerosol species, and how they compare with the effect of doubling CO_2. Our main conclusions are:

[42] 1. The temperature response of the model to forcing by biomass-burning is quite different from the hemispherically asymmetric response to sulfate and black carbon aerosols, both of which have their responses concentrated in the northern hemisphere, especially at high latitudes. The different spatial pattern of the response to biomass-burning aerosols has implications for detection/attribution studies.

[43] 2. Changes in precipitation appear be driven by inter-hemispheric temperature changes, with an asymmetric

warming/cooling in the northern hemisphere leading to a northward/southward shift of the ITCZ.

[44] 3. The efficacy of forcing by sulfate and black carbon aerosols is found to be similar to that obtained in studies with a previous Hadley Centre model [*Williams et al.*, 2001; *Roberts and Jones*, 2004].

[45] 4. Changes in sea-salt aerosol are related to changes in sea-ice cover and wind speed, whereas the response of mineral dust is mainly dependent on changes in soil moisture.

[46] 5. Additivity of response seems to hold for the changes in near-surface temperature and precipitation. This suggests that individual forcing mechanisms can be studied and the response approximated by a linear sum of these individual responses without running a large set of model experiments with the various combinations of forcings. Detailed feedback may, however, be non-linear, and further work is required to assess whether this additivity extends to non-aerosol forcings in our model.

[47] **Acknowledgments.** We would like to thank Prof. D. B. Stephenson for statistical advice. This work was supported by the UK Department for the Environment, Food and Rural Affairs under contract PECD 7/12/37.

References

Albrecht, B. A. (1989), Aerosols, cloud microphysics, and fractional cloudiness, *Science*, *245*, 1227–1230.

Bellouin, N., O. Boucher, J. M. Haywood, C. E. Johnson, A. Jones, J. G. L. Rae, and S. Woodward (2007), Improved representation of aerosolsfor HadGEM2, Hadley Centre Tech. Note, No. 73. (Available at http://www.metoffice.gov.uk/research/hadleycentre/pubs/HCTN/index.html)

Biasutti, M., and A. Giannini (2006), Robust Sahel drying in response to 20th century forcings, *Geophys. Res. Lett.*, *33*, L11706, doi:10.1029/2006GL026067.

Dentener, F., et al. (2006), Emissions of primary aerosol and precursor gases in the years 2000 and 1750 prescribed data-sets for AeroCom, *Atmos. Chem. Phys.*, *6*, 4321–4344.

Forster, P. M. de F., and K. E. Taylor (2006), Climate forcings and climate sensitivities diagnosed from coupled climate model integrations, *J. Clim.*, *19*, 6181–6194.

Forster, P., et al. (2007), Changes in atmosphericconstituents and in radiative forcing, in *Climate Change 2007: The Physical Science Basis. Contribution of Working Group I to the Fourth Assessment Report of the Intergovernmental Panel on Climate Change*, edited by S. Solomon, D. Qin, M. Manning, Z. Chen, M. Marquis, K. B. Averyt, M. Tignor, and H. L. Miller, pp. 129–234, Cambridge Univ. Press, Cambridge, UK, and New York, USA.

Gillett, N. P., M. F. Wehner, S. F. B. Tett, and A. J. Weaver (2004), Testing the linearity of the response to combined greenhouse gas and sulfate aerosol forcing, *Geophys. Res. Lett.*, *31*, L14201, doi:10.1029/2004GL020111.

Hansen, J., M. Sato, and R. Ruedy (1997), Radiative forcing and climate response, *J. Geophys. Res.*, *102*, 6831–6864.

Hansen, J., et al. (2005), Efficacy of climate forcings, *J. Geophys. Res.*, *110*, D18104, doi:10.1029/2005JD005776.

Haywood, J. M., R. J. Stouffer, R. T. Wetherald, S. Manabe, and V. Ramaswamy (1997), Transient response of a coupled model to estimated changes in greenhouse gas and sulfate concentrations, *Geophys. Res. Lett.*, *24*, 1335–1338.

IPCC (2007), *Climate Change 2007: The Physical Science Basis. Contribution of Working Group I to the Fourth Assessment Report of the Intergovernmental Panel on Climate Change*, edited by S. Solomon, D. Qin, M. Manning, Z. Chen, M. Marquis, K. B. Averyt, M. Tignor, and H. L. Miller, Cambridge Univ. Press, Cambridge, UK, and New York, USA.

Jacobson, M. Z. (2002), Control of fossil-fuel particulate black carbon and organic matter, possibly the most effective method of slowing global warming, *J. Geophys. Res.*, *107*(D19), 4410, doi:10.1029/2001JD001376.

Jacobson, M. Z. (2004), Climate response of fossil fuel and biofuel soot, accounting for soot's feedback on snow and sea ice albedo and emissivity, *J. Geophys. Res.*, *109*, D21201, doi:10.1029/2004JD004945.

Johns, T. C., et al. (2006), The new Hadley Centre climate model (HadGEM1): Evaluation of coupled simulations, *J. Clim.*, *19*, 1327–1353.

Jones, A., D. L. Roberts, M. J. Woodage, and C. E. Johnson (2001), Indirect sulphate aerosol forcing in a climate model with an interactive sulphur cycle, *J. Geophys. Res.*, *106*, 20,293–20,310.

Lohmann, U., and J. Feichter (2005), Global indirect aerosol effects: A review, *Atmos. Chem. Phys.*, *5*, 715–737.

Martin, G. M., M. A. Ringer, V. D. Pope, A. Jones, C. Dearden, and T. J. Hinton (2006), The physical properties of the atmosphere in the new Hadley Centre Global Environment Model (HadGEM1). Part I: Model description and global climatology, *J. Clim.*, *19*, 1274–1301.

Penner, J. E., S. Y. Zhang, and C. C. Chuang (2003), Soot and smoke aerosol may not warm climate, *J. Geophys. Res.*, *108*(D21), 4657, doi:10.1029/2003JD003409.

Ramaswamy, V., and C.-T. Chen (1997), Linear additivity of climate response for combined albedo and greenhouse perturbations, *Geophys. Res. Lett.*, *24*, 567–570.

Ramaswamy, V., O. Boucher, J. Haigh, D. Hauglustaine, J. Haywood, G. Myhre, T. Nakajima, G. Y. Shi, and S. Solomon (2001), Radiative forcing of climate change, in *Climate Change 2001: The Scientific Basis, Contribution of Working Group I to the Third Assessment Report of the Intergovernmental Panel on Climate Change*, edited by J. T. Houghton, Y. Ding, D. J. Griggs, M. Noguer, P. J. van der Linden, X. Dai, K. Maskell, and C. A. Johnson, Cambridge Univ. Press, Cambridge, UK.

Roberts, D. L., and A. Jones (2004), Climate sensitivity to black carbon aerosol from fossil fuel combustion, *J. Geophys. Res.*, *109*, D16202, doi:10.1029/2004JD004676.

Rotstayn, L. D., and U. Lohmann (2002), Tropical rainfall trends and the indirect aerosol effect, *J. Clim.*, *15*, 2103–2116.

Rotstayn, L. D., and J. E. Penner (2001), Indirect aerosol forcing, quasi forcing, and climate response, *J. Clim.*, *14*, 2960–2975.

Senior, C. A., and J. F. B. Mitchell (1993), Carbon dioxide and climate: The impact of cloud parameterization, *J. Clim.*, *6*, 393–418.

Sexton, D. M. H., H. Grubb, K. P. Shine, and C. K. Folland (2003), Design and analysis of climate model experiments for the efficient estimation of anthropogenic signals, *J. Clim.*, *16*, 1320–1336.

Smith, S. J., R. Andres, E. Conception, and J. Lurz (2004), Historical sulfur dioxide emissions 1850–2000: Methods and results, *PNNL*, JGCRI Report, PNNL-14537. (Available at http://globalchange.umd.edu)

Sokolov, A. (2006), Does model sensitivity to changes in CO_2 provide a measure of sensitivity to other forcings?, *J. Clim.*, *19*, 3294–3306, doi:10.1175/JCLI3791.1.

Twomey, S. A. (1974), Pollution and the planetary albedo, *Atmos. Environ.*, *8*, 1251–1256.

Williams, K. D., A. Jones, D. L. Roberts, C. A. Senior, and M. J. Woodage (2001), The response of the climate system to the indirect effects of anthropogenic sulfate aerosol, *Clim. Dyn.*, *17*, 845–856.

Woodward, S. (2001), Modelling the atmospheric life-cycle and radiative impact of mineral dust in the Hadley Centre climate model, *J. Geophys. Res.*, *106*, 18,155–18,166.

O. Boucher, J. M. Haywood, and A. Jones, Met Office Hadley Centre, FitzRoy Road, Exeter, EX1 3PB, UK. (olivier.boucher@metoffice.gov.uk; jim.haywood@metoffice.gov.uk; andy.jones@metoffice.gov.uk)